Microscopic Origin of Surface-Plasmon Radiation in Plasmonic Band-Gap Nanostructures

D. S. Kim,[1] S. C. Hohng,[1] V. Malyarchuk,[2] Y. C. Yoon,[1] Y. H. Ahn,[1] K. J. Yee,[1] J. W. Park,[3] J. Kim,[3] Q. H. Park,[4] and C. Lienau[2]

[1]*School of Physics, Seoul National University, Seoul 151-742, Korea*
[2]*Max-Born-Institut für Nichtlineare Optik und Kurzzeitspektroskopie, D-12489 Berlin, Germany*
[3]*Korea Research Institute of Standards and Science, Yusung, Taejon 305-600, Korea*
[4]*Department of Physics, Korea University, Seoul 136-701, Korea*

(Received 22 July 2002; published 30 September 2003)

We report spatial domain measurements of the damping of surface-plasmon excitations in metal films with periodic nanohole arrays. The measurements reveal a short coherent propagation length of a few μm inside nanohole arrays, consistent with delays of about 10 fs in ultrafast transmission experiments. This implies that the transmission spectra of the entire plasmonic band-gap structure are homogeneously broadened by radiative damping of surface-plasmon excitations. We show that a Rayleigh-like scattering of surface plasmons by the periodic hole array is the microscopic origin of this damping, allowing the reradiation rate to be controlled.

DOI: 10.1103/PhysRevLett.91.143901 PACS numbers: 42.70.Qs, 07.79.Fc, 42.25.–p, 73.20.Mf

The optical properties of metal films perforated with regular subwavelength hole arrays have been of considerable experimental and theoretical interest, ever since Ebbesen *et al.* [1] discovered that these structures allow unusually high transmission of light at surface-plasmon (SP) resonances [1–6]. Phenomenologically, the incident light is grating coupled to SP excitations on the metal interfaces. SPs on either side of the metal film are coupled through the nanoholes and may eventually be reemitted into far-field radiation. This enhances the on-resonance transmission by 2–3 orders of magnitude over that of isolated nanoapertures, giving rise to a wide range of possible applications, e.g., as near-field sources, in photonic integrated circuits, or in lithography [1,7].

The optical properties of subwavelength hole arrays can be described by eigenvalue solutions of Maxwell's equation in a periodic dielectric medium [8,9]. The real and imaginary part of the eigenvalues reflect the energy positions of the transmission resonances and the damping of the Bloch states, i.e., the eigenvectors, respectively. The spectral resonances have been investigated [2] and energy gaps in the dispersion were observed [1]. Much less is known about the electric field profiles at the metal interfaces and about the damping of SP excitations in nanohole arrays, i.e., about the microscopic origin of the line shapes of the transmission spectra. Such information is important for understanding the underlying physics and for optimizing such nanostructures for possible applications. Here, near-field optical techniques are powerful tools, as they allow for direct mapping of the eigenmodes of subwavelength structures and their damping rates.

In this Letter we directly measure the damping of SP excitations in periodic nanohole arrays. By showing that coherent spatial SP propagation lengths are a few μm and ultrafast decay of the SP polarization occurs on a 10 fs time scale, we demonstrate that the SP transmission peaks are homogeneously broadened by the SP radiative lifetime. The pronounced dependence of the damping rate on wavelength and hole size shows that the microscopic origin of the conversion of SP into light is Rayleigh-like scattering by the periodic hole array.

Nanohole arrays are fabricated by dry etching after *e*-beam patterning on a 300 nm thick gold film grown on a $\lambda/5$ flat sapphire substrate. The optical axis of the substrate is perpendicular to the metal surface to avoid any effects of birefringence. The initial experiments are performed on a sample with a hole radius r of 125 nm and a period a_0 of 761 nm of the square array. Its far-field emission spectrum [Fig. 1(a)] shows transmission peaks assigned to SP resonances at either the air-metal (AM) or sapphire-metal (SM) interfaces. For each interface, the resonances $[p, q]$ correspond to grating momenta $\tilde{\Delta}k = (p, q)2\pi/a_0$ transferred to the incident beam [2]. The peak at 827 nm is assigned to the AM $[1, 0]$ or $[0, 1]$ mode and that at 925 nm is the SM $[1, 1]$ resonance. We use a near-field scanning optical microscope (NSOM) in transmission geometry. The sample is illuminated with linearly polarized light from a Ti:sapphire laser through

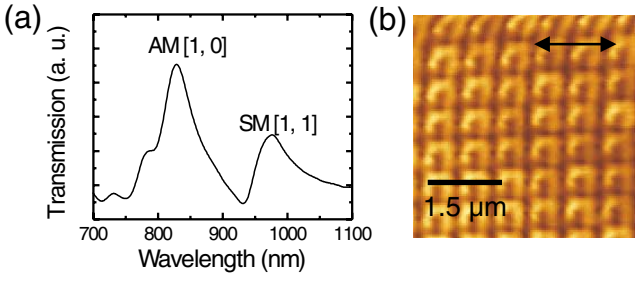

FIG. 1 (color). (a) Transmission spectrum of a gold nanohole array with $a_0 = 761$ nm and $r = 125$ nm. (b) Near-field transmission image at an excitation wavelength of 820 nm.

the substrate and the electric field intensity at the metal-air interface is coupled into a metal-coated near-field probe with sub-100 nm aperture diameter.

In Fig. 1(b), the near-field emission pattern at an excitation wavelength of 820 nm near the AM $[1, 0]$ resonance within a scan range of about $5 \times 5\ \mu m^2$ is plotted. The emission pattern has the same periodicity as the nanohole array. It reflects the field intensity of the excited Bloch states at the metal-air interface and is given as a coherent superposition of SP waves with wave vectors $(k_x, k_y) = \frac{2\pi}{a_0}(m, n)$, where m, n are integers. Fourier transforms indicate that only a few of the lowest order Bloch waves $(m, n) \leq 2$ are detected for samples with hole radii of more than 100 nm. For probing SP damping it is important that these experiments verify that SP modes are efficiently excited at the metal-air interface [10] and that these modes are detected with high spatial resolution with the NSOM. This conclusion is confirmed by the agreement between experimental near-field images and 3D finite difference time domain simulations [10].

To measure the damping of SP excitations, we first probe their spatial propagation length, employing the experimental geometry shown in Fig. 2(a). The AM $[1, 0]$ SP mode is excited at the metal-air interface of the first nanohole array. This mode is scattered at the edge of the array, and a significant fraction of this mode is transmitted to the flat gold surface. On the flat metal, the SP propagation length is on the order of 40 μm [11]. When these waves encounter a second hole pattern with the same period a_0, they are scattered at the nanoholes. Interference of multiply scattered SP waves gives rise to an intensity pattern I_{SP}, whose spatial variation along the x axis is sensitive to both damping of the amplitude of the SP mode (characteristic time τ) and to purely phase disturbing scattering processes (characteristic time T_2^* [12]). Damping leads to a spatial decay of the field intensity, whereas pure dephasing processes would lead to a change in the image contrast. Shown in Figs. 2(b) and 2(c) are $5 \times 5\ \mu m^2$ scans of I_{SP} at excitation wavelengths of 760 and 830 nm, respectively. Both images reveal periodic pattern formation through interference of Bloch waves. As we probe deeper into the grating, the spatial pattern remains unchanged but its overall intensity shows a rapid decay, decreasing by more than an order of magnitude within 5 μm. This demonstrates that there is a strong SP damping on a length scale that is substantially shorter for hole arrays than on high-conductivity metal surfaces. Intensity profiles $\int I_{SP} dy$, integrated along the y axis, are presented in Fig. 3(a) for excitation wavelengths of 760 and 830 nm. Both curves show, on average, an exponential decay $I_{SP} \propto \exp(-2x/l_p)$ with propagation lengths of 2.68 and 3.26 μm, respectively.

For propagation of a plane wave through a dissipative medium, the damping time τ_p of the wave and the propagation length l_p are linked through $\tau_p = l_p/v_{ph}$ where v_{ph} is the phase velocity of SP. In our sample, a_0 is 761 nm and the AM $[1, 0]$ mode has its peak at 827 nm. Therefore, v_{ph} can be estimated as $\frac{761}{827} c \simeq 0.92c$, where c is the speed of light. We then deduce SP damping times τ_p of 9.7 and 11.8 fs, respectively.

To confirm the equivalence between spatial propagation and temporal damping of the SP excitation, we perform a direct measurement of the SP damping in the time domain. We measure the noncollinear intensity cross

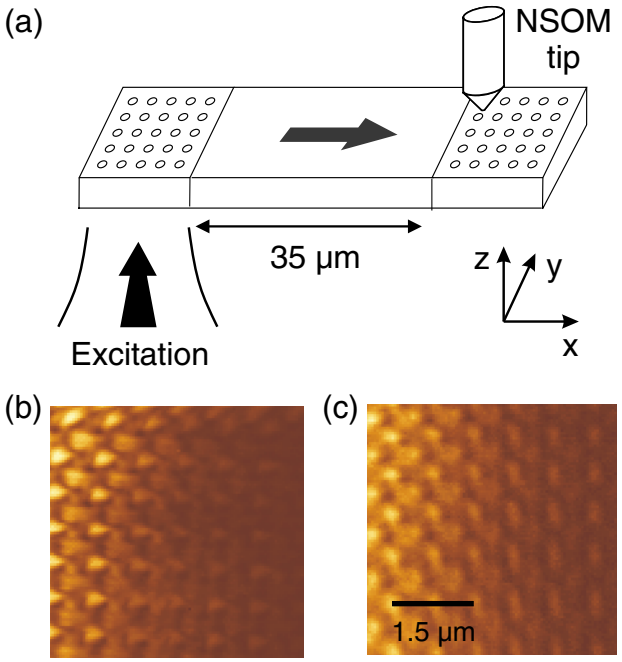

FIG. 2 (color). (a) Schematics of the experiment. The incident polarization is along x, the SP propagation direction (arrow). (b),(c) Near-field images of the intensity $I_{SP}(x, y)$ on the nonilluminated grating side within a scan area of $5 \times 5\ \mu m^2$. The excitation was at 760 nm (b) and 830 nm (c), close to the AM $[1, 0]$ resonance (790 nm) .

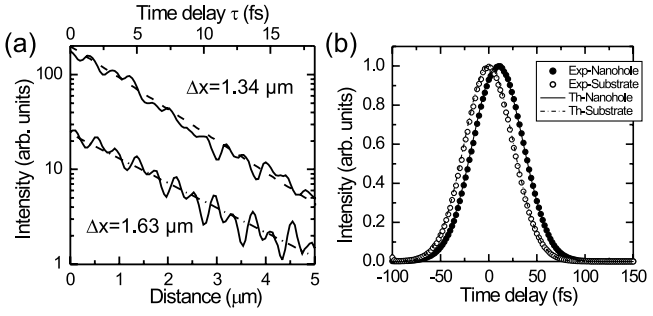

FIG. 3. (a) Decay of $\int I_{SP}(x, y) dy$ of Figs. 2(b) and 2(c), versus distance x. The excitation was at 760 nm (top) and 830 nm (bottom). Dashed line: exponential decay. (b) Top (experiment): cross correlations of fs pulse transmission ($\lambda =$ 790 nm) through a nanohole array (filled circles) and through the substrate only (open circles). Solid line: curve calculated from Eq. (1) assuming $\tau = 10$ fs.

correlation of a 40 fs pulse transmitted through the sample with a replica of the incident pulse [13]. The laser is centered at 790 nm. Figure 3(b) (top curve) compares cross correlations recorded for transmission through the nanohole array (solid line) and through the substrate only (dotted line), respectively. A clear time delay of 10 ± 1 fs is observed, when the pulse is transmitted through the nanohole structure. To interpret these experiments, we use a simplified, physically intuitive picture. The incident pulse $E_{\text{in}}(t)$ drives the AM $[1, 0]$ mode polarization P_{SP} near the resonance frequency ω_{SP}. We describe the dynamics of P_{SP} by a driven harmonic oscillator equation

$$\frac{d^2P_{\text{SP}}}{dt^2} + \frac{2}{\tau}\frac{dP_{\text{SP}}}{dt} + \omega_{\text{SP}}^2 P_{\text{SP}} \propto E_{\text{in}}(t). \quad (1)$$

All transmitted light is assumed to originate from SP radiation. Since $T_2^* \gg \tau$, the transmitted intensity $I_{\text{tr}}(t)$ is directly proportional to $|P_{\text{SP}}(t)|^2$. The finite damping of the polarization with τ then gives rise to a delay in the reemission of the SP field.

The experimental results are compared to a simulation based on Eq. (1), taking a Gaussian profile for the 40 fs input pulse. Good agreement with experiment is obtained if a SP damping time $\tau_d = 10$ fs is assumed. This damping time $\tau_d = 10$ fs of the total SP polarization matches well the values of $\tau_p = 9.7$ and 11.8 fs found for excitation wavelengths of 760 and 790 nm in the propagation experiments. This indicates strongly that it is indeed the finite damping of the driven SP resonance that is responsible for the delay in light transmission.

We now relate the measured damping times to the line shape of the SP resonances in the optical far-field transmission spectra. These spectra are recorded with a spatial resolution of 1 mm, i.e., much larger than the coherent SP propagation length l_p of few μm. Hence, both homogeneous and inhomogeneous broadening may contribute to the far-field line shape. In the absence of inhomogeneous broadening the homogeneous linewidth of a single Lorentzian resonance is $\Gamma = 2\hbar/\tau$, where τ is the total damping time. In our sample, the AM $[1, 0]$ mode has a FWHM of $\Gamma = 140$ meV, corresponding to $\tau = 9.4$ fs. From the measured $\tau_p = 9.7$ and 11.8 fs, we calculate line widths of 135 and 112 meV. Therefore, SP damping can account for most of the measured linewidth in the far-field transmission spectra. This indicates that contributions from inhomogeneous broadening arising from structural imperfections are of minor importance and that the system can be considered to be homogeneously broadened. This equivalence between spectral linewidth and SP damping has been confirmed for different resonances and samples.

Insight into the microscopic origin of the SP damping can be obtained from the propagation experiments. They suggest that Γ is mostly limited by radiative SP decay into light through scattering at the nanoholes. Such scattering should well be described by classical Mie theory in the Rayleigh limit $a_0 \ll \lambda$. For Rayleigh scattering of 3D waves by small spheres, the pronounced wavelength and radius dependence of the scattering cross section $\sigma \propto r^6/\lambda^4$ is well known. Scattering of quasi-2D surface bound waves by single circular apertures has only recently been studied theoretically [14]. An r^4 dependence of σ has been predicted, as expected for dipole scattering. We are, however, not aware of a theoretical model for the wavelength and hole size dependence of SP damping in nanohole arrays.

To show that the SP damping is indeed dominated by Rayleigh scattering, we first study the wavelength dependence of the spectral line widths. Figure 4(a) plots, on a double logarithmic scale, the widths Γ of the individual SP resonances of four samples with similar hole radii (open circles) [15]. Widths deduced from time delay and propagation measurements are shown as filled triangles and filled circles, respectively. We find that Γ scales as λ^n with $n = -3.4 \pm 0.5$. This is indicative of Rayleigh scattering, yet the data show considerable scatter, making a final judgment difficult. This scatter is not surprising, as the damping of different AM and SM SP eigenmodes is compared. Mode dependent scattering amplitudes give rise to variation in Γ among the different resonances. We thus probe the wavelength-dependent linewidth of a single resonance by measuring angle-dependent transmission spectra near the SM $[1, 0]$ resonance [Fig. 4(b), inset]. Figure 4(b) shows the power-law scaling of Γ and we now find a slope $n = 4.2 \pm 0.3$, demonstrating that the scattering mechanism is indeed Rayleigh-like. Note that the narrow linewidth of only 15 meV around 1.8 μm

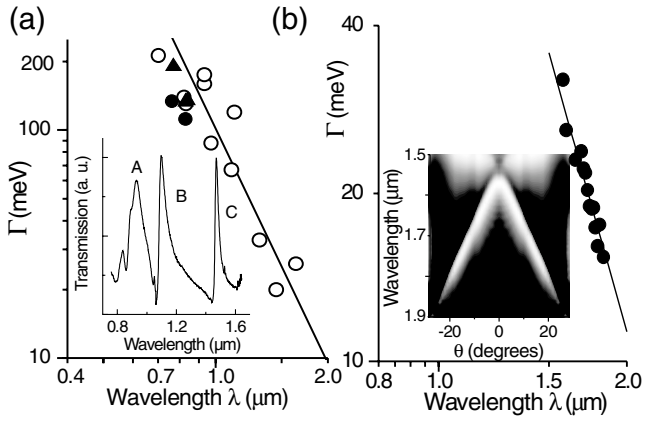

FIG. 4. (a) Log-log plot of line widths Γ versus peak wavelengths λ for different nanohole arrays with $r = 125$ nm. The solid line is a fit of Γ to λ^{-n}, with $n = 3.4$. Inset: transmission spectrum for a gold sample with $a_0 = 800$ nm and $r = 125$ nm. *A*, *B*, and *C* correspond to AM $[1, 0]$, SM $[1, 1]$, and SM $[1, 0]$ resonances. (b) Γ vs λ for various incident angles for the SM $[1, 0]$ peak and fit to λ^{-4} (line). Inset: transmission spectra of the SM $[1, 0]$ resonance as a function of incident angle θ.

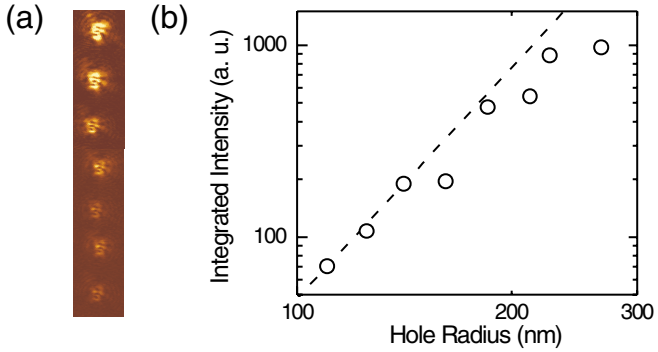

FIG. 5 (color). (a) Far-field emission patterns from various single holes with radii decreasing from 267 nm (top) to 110 nm (bottom). The images are recorded at a tip-to-sample distance of 0.6 μm. (b) Log-log plot of the spatially integrated emission intensity around the single holes plotted against their hole radius r. The dotted line is a fit to the fourth power of r.

corresponds to a τ of 90 fs and a coherent propagation length of $l_p = 25$ μm, i.e., about 30 lattice periods.

This conclusion is fully supported by the hole size dependence of the SP scattering cross section. A row of eight nanoholes, separated by 10 μm, is placed at a distance of 50 μm from a periodic nanohole array. Similar to Fig. 2(a), SP waves are generated in the periodic hole array, propagate over 50 μm across the flat metal surface, and are scattered at the single nanoholes. In the near field, interference patterns of incident and scattered SPs are formed and detected. At a tip-to-sample distance of 0.6 μm, however, these evanescent SP modes are not observed and only the photons scattered into the far field are collected. We find a drastic decrease in emission intensity by a factor of 30 as r is decreased from 267 to 110 nm [Fig. 5(a)]. Indeed, the double logarithmic plot in Fig. 5(b) shows for small radii the predicted r^4 dependence. For the large radii a weaker dependence is observed, most likely reflecting that here the Rayleigh limit is no more applicable. The results show clearly that the damping time τ of SP excitations in these nanohole arrays is limited by the finite SP lifetime $T_1 \simeq \tau/2$ due to Rayleigh scattering into far-field radiation. Pure dephasing processes, reflecting phase fluctuations without population decay, are negligible. Also Ohmic losses due to nonradiative SP decay into phonons play only a minor role. Hence, the SP lifetime is substantially shorter than on high-conductivity metal surfaces, where nonradiative losses may dominate [11,16]. The radiative damping mechanism in nanohole arrays is similar to that in metal nanoparticles [12,17], yet here the damping times are much shorter, giving rise to line widths of several hundreds of meV. The possibility to tailor the damping rate in nanohole arrays by varying the hole radius and distance is relevant for applications.

In conclusion, we have experimentally studied the damping of surface-plasmon excitations in metallic nanohole arrays. By relating nanoscopic SP propagation, ultrafast light transmission, and optical spectra, we demonstrate that the transmission spectra of these plasmonic band-gap structures are homogeneously broadened. The spectral line shape and damping time are dominated by Rayleigh scattering of SP into light and can be varied by controlling the resonance energy and/or hole radius. This opens the way toward designing SP nanooptic devices and spatially and spectrally tailoring light-matter interactions on nanometer length scales.

We thank J. J. Baumberg, S. T. Cundiff, and J. J. Greffet for helpful discussions. Financial support of the work in Korea by MOST (NRL and Nano-Photonics program) and KOSEF (SRC program) and that in Germany by the DFG (SFB296) and by the EU (EFRE and SQID) is gratefully acknowledged.

[1] T.W. Ebbesen *et al.*, Nature (London) **391**, 667 (1998).
[2] H. F. Ghaemi *et al.*, Phys. Rev. B **58**, 6779 (1998).
[3] U. Schröter and D. Heitmann, Phys. Rev. B **58**, 15 419 (1998).
[4] J. A. Porto, F. J. Garcia-Vidal, and J. B. Pendry, Phys. Rev. Lett. **83**, 2845 (1999).
[5] L. Salomon *et al.*, Phys. Rev. Lett. **86**, 1110 (2001).
[6] L. Martin-Moreno *et al.*, Phys. Rev. Lett. **86**, 1114 (2001).
[7] S. I. Bozhevolnyi *et al.*, Phys. Rev. Lett. **86**, 3008 (2001).
[8] M. M. J. Treacy, Appl. Phys. Lett. **75**, 606 (1999).
[9] J. D. Joannopoulos, R. D. Meade, and J. N. Winn, *Photonic Crystals* (Princeton University, Princeton, 1995).
[10] S. C. Hohng *et al.*, Appl. Phys. Lett. **81**, 3239 (2002).
[11] B. Lamprecht *et al.*, Appl. Phys. Lett. **79**, 51 (2001).
[12] C. Sonnichsen *et al.*, Phys. Rev. Lett. **88**, 077402 (2002).
[13] A. Dogariu *et al.*, Opt. Lett. **26**, 450 (2001).
[14] A.V. Shchegrov, I.V. Novikov, and A. A. Maradudin, Phys. Rev. Lett. **78**, 4269 (1997).
[15] The Γ values in Fig. 4 are taken as the FWHM of the SP resoances in the far-field spectra. The λ^{-4} dependence is confirmed by a full line shape analysis, in which the low-energy part of the SP resonance is fitted to a Lorentzian.
[16] M. van Exter and A. Lagendijk, Phys. Rev. Lett. **60**, 49 (1987).
[17] T. Klar *et al.*, Phys. Rev. Lett. **80**, 4249 (1998).